Journal of Materials Chemistry A

Accepted Manuscript

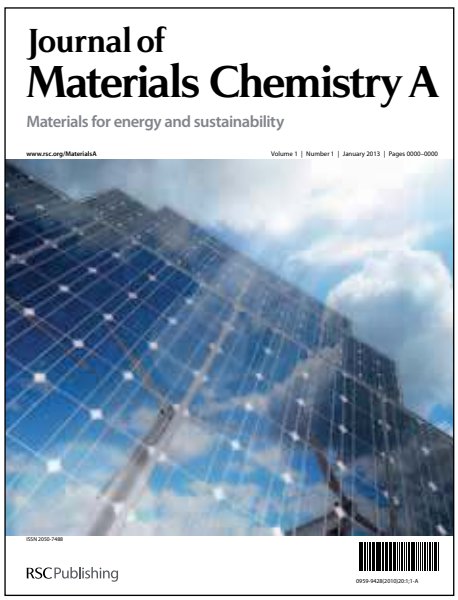

RSC Publishing

www.rsc.org/materialsA
Registered Charity Number 207890

Journal of Materials Chemistry

Dynamic Article Links ►
View Article Online

Cite this: DOI: 10.1039/c0xx00000x

www.rsc.org/xxxxxx

Full Paper

Open Circuit Voltage tuning through molecular design in Hydrazone end capped donors for Bulk Heterojunction solar cells.

Mauro Sassi,[a] Maurizio Crippa,[a] Riccardo Ruffo,[a] Riccardo Turrisi,[a] Martin Drees,[b] Upendra K. Pandey,[c] Roberto Ter-mine,[c] Attilio Golemme,[c] Antonio Facchetti[b] and Luca Beverina[a]*

Received (in XXX, XXX) Xth XXXXXXXXX 20XX, Accepted Xth XXXXXXXXX 20XX
DOI: 10.1039/b000000x

The design, synthesis and characterization of five diphenylhydrazone end capped molecules as Donors for Bulk Heterojunction (BHJ) solar cells are described. The use of the Hydrazone donor instead of the more common amine one is advantageous in terms of synthetic access and overall stability. We show that the variation of both the nature and the substitution pattern of the electron deficient conjugated bridge enables the tuning of the optical energy gap as well as of the HOMO and LUMO. In particular, our data show that the low energy shift of the HOMO level along the series of hydrazone compounds, one of the critical parameters affecting the performances of BHJ cells, is as high as 0.42 eV. We tested all derivatives as Donors in a BHJ configuration, using the fullerene derivative [6,6]-phenyl-C_{71}-butyric acid methyl ester ($PC_{71}BM$) as the acceptor. We found that the trend we observed in the progressive stabilization of the chromophore HOMO level upon increasing the electron accepting capabilities of the conjugated bridge is reflected in the progressive increase of the cell Open Circuit Voltage (Voc). Our preliminary results show that it is possible to obtain an Voc as high as 0.74 V, along with a power conversion efficiency of 1.2 %.

Introduction.

Small molecule semiconductors are gaining attention as efficient Donors for Organic photovoltaic cells based on the Bulk Heterojunction (BHJ) concept.[1-3] In its most common embodiment, the active layer of a BHJ cell consists in a blend of an electron rich derivative, the Donor, and an electron poor one, the Acceptor.[4] The two derivatives need - upon evaporation of the deposition solvent or solvent mixture - to give rise to a spontaneous phase separation into interpenetrated domains, with typical dimensions in the tens of nanometers range. Such a solid-state arrangement is preferred when one of the two components of the mixture is a polymer (most commonly the Donor) and the other (the fullerene Acceptor) is a small molecule.[5] Polymer-based BHJ solar cells provide the best performances in terms of Power Conversion Efficiency (PCE).[6-8] However, the use of polymeric conjugated derivatives suffers from two important drawbacks. The first one is the intrinsic polydispersed nature of polymeric materials, sometimes affecting reproducibility.[9] The second one deals with the purification issues connected with the inapplicability of sublimation on such substrates. As a consequence, recent literature reports on a number of more or less efficient low molecular weight Donor materials, used with the common $PC_{61}BM$ or $PC_{71}BM$ acceptors.[3] Amongst the most efficient classes of proposed materials are diketopyrrolopyrroles,[10-13] oligothiophenes,[14-16] squaraines,[17-19] merocianies,[20] phthalocyanines[21,22] and combinations of such compounds.[23]

From the standpoint of the design guidelines, the ideal molecular Donor should have: 1) a LUMO level ~ 0.3 eV above the LUMO of the Acceptor, thus enabling photoinduced electron transfer; 2) a broad absorption extending over the best part of the visible spectrum, particularly regarding to the low energy portion where the fullerene acceptor does not absorb; 3) A low lying HOMO level. In fact, the maximum voltage that a BHJ cell can generate (the so called open circuit voltage Voc) is directly connected with the difference in energy between the HOMO level of the donor material and the LUMO level of the acceptor. In recent years, the design of both molecular and polymeric efficient Donors relied on the exploitation of alternating Electron rich and Electron poor groups along a conjugation axis. The establishment of efficient charge transfer transitions provides, at the same time, large extinction coefficients and broad absorption bands. The electron rich groups mostly are alkoxy substituents, amines or π-excessive heterocycles like thiophene, oxazole and furane. The electron poor residue can be a π-deficient heterocycle or a strongly electron withdrawing moiety like the cyano or a carbonyl group. Recently, we proposed hydrazones as efficient Donors, on the basis of three main characteristics of this peculiar functionality that are relevant to OPV devices: 1) Easy synthetic access, as hydrazones can be readily obtained from carbonylic compounds, mostly aldehydes; 2) With respect to the corresponding amines, hydrazones are at the same time more conjugated, thus ensuring narrow optical gaps, and less pronouncedly electron donating, with consequences on the position of HOMO and LUMO levels; 3) Hydrazones are typically highly thermally and chemically stable.

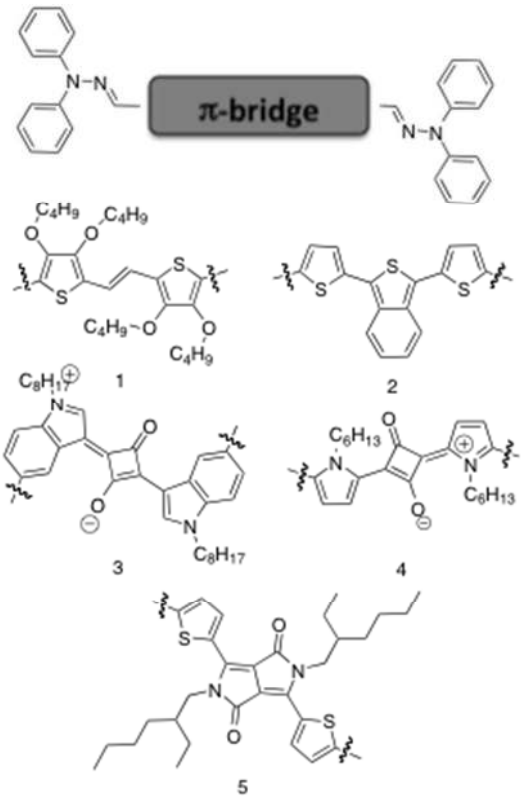

Scheme 1.

So far, we exploited hydrazone end capped derivatives with a dipyrrolosquarilium core as an electron accepting bridge. In particular, we demonstrated that a 1:3 by weight blend of the end-capped hydrazone squaraine **4** (Scheme 1) with $PC_{71}BM$ afforded a PCE as high as 1.49 %, along with a Voc of 0.55 V.[24] We have shown that the introduction of a number of different electron withdrawing substituents on the hydrazone moiety is an efficient strategy to control both the HOMO and LUMO energies, thus in principle enabling the further optimization of final performances. Indeed, we were able to demonstrate an increase of 0.3 V in the measured Voc.[18] Unfortunately, the substitution process negatively affected the morphology, thus leading to efficiencies generally lower than 1 %. The aim of the present paper is to explore the capabilities of the simple, unsubstituted diphenylhydrazone moiety to act as a performing donor in D-A-D molecules possessing accepting (A) bridges with different electron accepting capabilities. In particular, we selected two of the most efficient acceptors reported in the literature, the isothionaphtene core (derivative **2**) and the diketopyrrolopyrrole core (derivative **5**). In derivative **3**, we introduced a different squarylium core, the diindolosquarilium. Finally, in derivative **1** we used an electron-donating core, the tetrabutoxydithienylethylene core, for comparison purposes. Scheme 1.

Experimental part.

1. Synthesis of the materials.

Scheme 1 shows the molecular structure of the diphenylhydrazone end-capped molecules we prepared. All derivatives are symmetric and can be prepared straightforwardly, according to the synthetic procedures shown in Scheme 2.

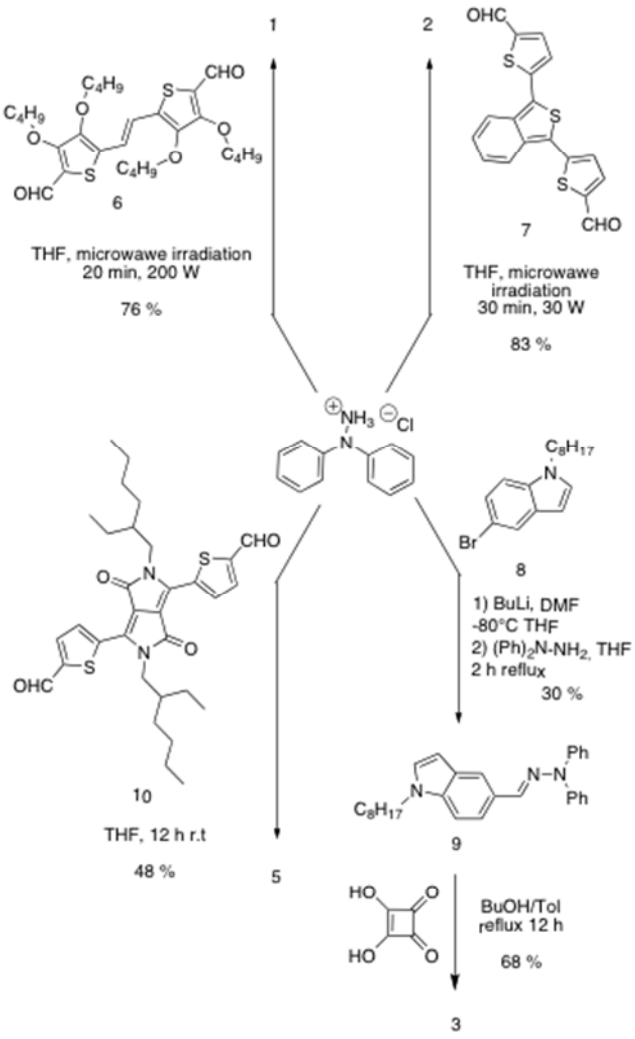

Scheme 2.

In details, derivative **1** is the only molecule possessing an electron donating bridge. Its synthesis was planned in order to compare the properties of an all donor compound with those of the D-A-D compounds possessing electron-accepting bridges of different accepting strength. Hydrazone **1** was prepared in high yield by the microwave enhanced (average power 200 W) condensation reaction of dialdehyde **6**[25] and diphenylhydrazine hydrochloride in THF in a sealed reaction tube. Chromatographic purification afforded analytical sample in good yield. The same procedure was also applied for the condensation of dialdehyde **7** with diphenylhydrazine hydrochloride. Due to the higher reactivity of the electron poor derivative **7** with respect to the electron-rich **6**, the reaction was in this case carried out under milder conditions (average power 40 W). The most electron poor dialdehyde in the series, the diketopyrrolopyrrole derivative **10**, was reactive enough to give compound **5** directly by simply stirring the suspension of reagents in THF overnight at room temperature.

A straightforward filtration through a pad of silica afforded directly the analytical sample in good yields.

Squaraine **3** was prepared starting from the n-octlyl-5-bromoindole **8**. Derivative **8** was firstly converted to the corresponding aldehyde by lithium-halogen exchange followed by quenching with DMF. The aldehyde was converted into the corresponding hydrazone **9** by reaction with diphenylhydrazine hydrochloride in refluxing THF. Finally, hydrazone **9** was reacted with squaric acid in a BuOH/toluene 1:1 mixture, under azeotropic removal of water by means of an efficient Dean-Stark trap. Squaraine **4** was obtained according to the literature procedure.[24]

2. UV-Vis Characterization.

Figure 1 shows the normalized absorption of compound **1-5** and Table 1 summarizes relevant UV-Vis absorption characterization data. Both the peak energy and the shape of the absorption band reflect the nature of the various conjugated bridges. Derivative **1** features the only electron rich bridge and as such its absorption lacks the charge transfer nature shared by all other compounds in the series. Coherently with its all donor nature, **1** has the widest optical gap in the series. On going from **1** to **2**, the optical gap is significantly reduced and the band shape becomes broader and featureless. Derivatives **3** and **4** exhibit the typical cyanine-like narrow and intense absorption. Derivative **4** shows the narrower optical gap of the series. Although derivative **3** possess the larger number of π-conjugated electrons in the series, the reduced conjugation provided by a 5-substituted indole derivative with respect to the 2,5-pyrrolic junction largely affects the optical gap. Finally, the optical gap of derivative **5** is intermediate between those of **3** and **4**. Its absorption band shows the vibronic replica progression typical of diketopyrrolopyrrole derivatives.[10]

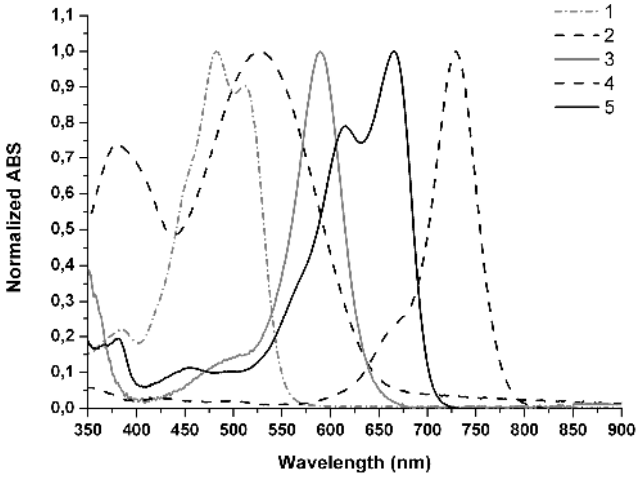

Figure 1. Normalized UV-Vis absorption of derivatives **1-5** in CH_2Cl_2.

From the stand point of its use in BHJ cells, the ideal Donor molecular derivative should possess a broad absorption extending over the whole visible spectrum, in particular at low energies, where the fullerene acceptor does not absorb. In this respect, derivatives **3-5** are the most promising candidates in terms of optical gap, whilst derivative **2** displays the broadest absorption in the series. Note that the absorption of squaraine compounds in the solid-state profits form a sizeable broadening due to strong charge transfer interaction between neighbouring molecules.[26]

Table 1. UV-Vis absorption characterization data for compounds 1-5 in $CHCl_3$.

Compound	λ_{max} (nm)	FWHM[a] (cm^{-1})	ε ($l\ cm^{-1}\ mol^{-1}$)
1	482	3843	25000
2	527	5507	55000
3	589	1628	170000
4	729	850	241000
5	666	2892	78000

[a]Full Width at Half the Maximum (FWHM)

3. Electrochemical Characterization.

All Derivatives possess similar electrochemical features. At oxidative potentials, the Cyclic Voltammetry (CV) curves show two oxidation waves attributed to the oxidation of the hydrazone moieties (Figure 2).

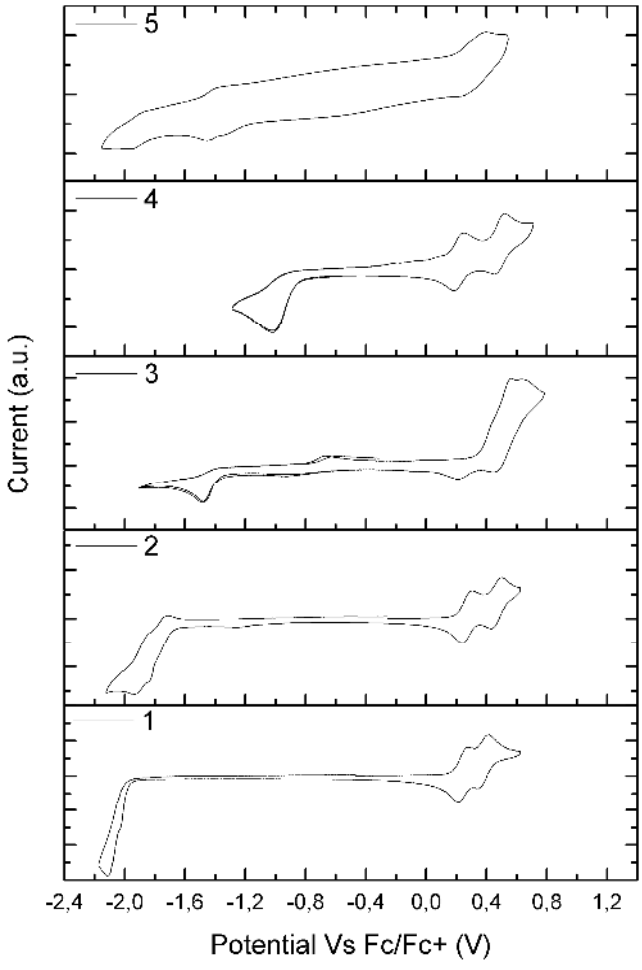

Figure 2. Cyclic Voltammetry plots of 10^{-4} M solution of derivatives **1-5** in tetrabuthylamonium hexafluorophosphate (TBAPF$_6$) 0.1 M in CH_3CN as the electrolyte and glassy carbon as the working electrode.

The first one corresponds to the formation of a delocalized radical cation, whilst the second is associated with the formation of the dication. Both the position and the potential separation between the two peaks can be used to probe the

electronic coupling between the end capping units and the electron-accepting core. Table 2 summarized the most relevant electrochemical data.

The electrochemical HOMO levels were estimated by considering the half wave potential of the first reversible oxidation peak for derivatives **1**,**2**,**4**. In the case of derivatives **3** and **5**, whose redox behavior is only partially reversible, the HOMO levels were obtained as the peak potential of the first oxidative wave of the corresponding Differential Pulse Voltammetry plot (see Supporting Information). The LUMO levels were obtained by subtracting the optical gap from the energy of the HOMO level.

According to the electron donating nature of its bridge, derivative **1** possesses a relatively high HOMO level. The potential separation between the two redox waves is rather large, thus indicating a high degree of coupling between the hydrazone end capping units. On going from **1** to derivative **2**, the HOMO level is downshifted by 120 meV whilst the peak separation slightly increases.

Table 2. Electrochemical HOMO and LUMO levels and peak potential separation (ΔE) between the fist and second oxidative wave for derivatives 1-5.

Compound	HOMO (eV)	LUMO (eV)	ΔE (meV)
1	-5.35	-2.78	140
2	-5.47	-3.12	197
3	-5.51	-3.40	121
4	-5.31	-3.61	280
5	-5.38	-3.52	85

This is in agreement with the proquinoidal nature of the isothionaphtene core, conveying efficient conjugation between the two hydrazone groups.[27] Derivatives **3**-**5** all possess π-accepting bridging groups. In particular, derivative **4** features the dipyrrolosquarilyum core we already exploited in the past in the context of photovoltaics.[24,17] Derivative **3** shares with **4** a squarylium core, but in this case we replaced pyrrole with indole. This heterocycle is intrinsically less pronouncedly electron rich than pyrrole. In addition, its particular regioselectivity in the electrophylic substitution reaction leads to a meta conjugation between the hydrazone end capping unit and the squarylium core.[28] The combination between the two effects leads to the particularly low-lying HOMO level of -5.51 eV. Finally, the HOMO level of the diketopyrrolopyrrole derivative **5** is intermediate between those of **3** and **4** and is placed at -5.38 eV.

Figure 3 shows a schematic representation of the energy levels diagram for all of the molecular donors and $PC_{71}BM$. Indeed, all the derivatives can in principle behave as Donor components in a BHJ cell, as in all cases the LUMO levels are higher than the $PC_{71}BM$ LUMO. The scheme also shows the progressive stabilization of the HOMO level on going from the all donor derivative **1** to the indolic squaraine **3**.

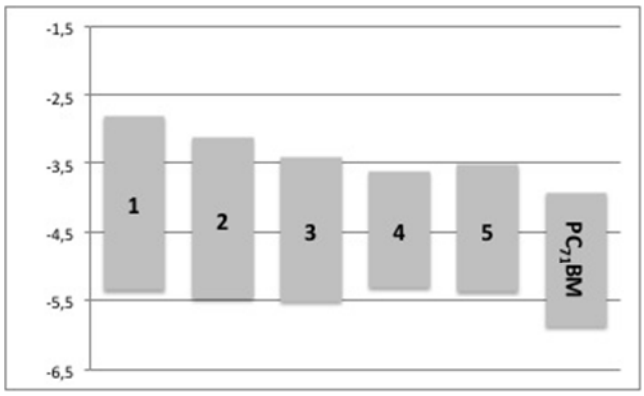

Figure 3. Schematic representation of the HOMO and LUMO levels of derivatives 1-5 with respect to those of the $PC_{71}BM$ acceptor.

4. Device assembly and testing.

We carried out OPV measurements for the newly synthetized derivatives and compared the results with those of the previously synthetized squaraine derivative **4**.

BHJ OPV devices were fabricated on PEDOT-coated ITO substrates using $PC_{71}BM$ as the acceptor. The cells based on derivatives **1** and **2** were fabricated and tested in a glow box under nitrogen atmosphere whilst cells based on derivatives **3**,**4** and **5** were fabricated in ambient atmosphere. After drying, the cells were then completed by sequential thermal evaporation of Ca and Al in the case of derivatives **1** and **2** and with sequential thermal vacuum deposition of LiF and Al in the case of derivatives **3**-**5**. We tested **1** and **2** based cells with LiF/Al cathodes as well but in this case we realized during device optimization that the power conversion efficiencies were sizably smaller than those obtained with Li/Al (See Table S1 of the Supporting Information). Table 3 contains the photovoltaic parameters of cells optimized in terms of several parameters, including Donor/Acceptor ratio, film thickness and solvent. In the case of derivative 2 the relatively large discrepancy between calculated and experimental value is attributed to the fact that EQE was obtained at lower total light intensity. Table S1 of the Supporting Information reports additional data. Figure 4a shows the J-V curves for BHJ cells based on blends of hydrazone derivatives **1**-**5** and $PC_{71}BM$. Figure 4b reports the corresponding External Quantum Efficiency plot for the corresponding cells.

Table 3. Photovoltaic properties of hydrazone based BHJ cells.

OPV Blend (w:w ratio)	Active layer thickness [nm]	J_{sc} [mA/cm^2]	V_{oc} [mV]	FF [%]	PCE [%]
1:$PC_{71}BM$ (1:3)	50	1.55[a] (1.89)[b]	580	32	0.35
2:$PC_{71}BM$ (1:3)	70	3.66[a] (2.69)[b]	620	35	0.59
3:$PC_{71}BM$ (1:3)	50	5.25[a] (4.70)[b]	680	36	1.16
4:$PC_{71}BM$ (1:3)	50	6.76[a] (7.10)[b]	560	37	1.49
5:$PC_{71}BM$ (1:3)	75	6.17[a] (5.68)[b]	710	35	1.53

[a] Corrected for EQE integration Experimental

The diphenylhydrazone moiety appears to be a valuable donating group; in fact all of the molecules we prepared show a HOMO level below -5.3 eV, significantly lower than that of P3HT (-5.0 eV). Such relatively low-lying HOMO translates in Voc values spanning from the 0.58 V of derivative **1** containing cells to the remarkable 0.74 V for derivative **5** containing cells.

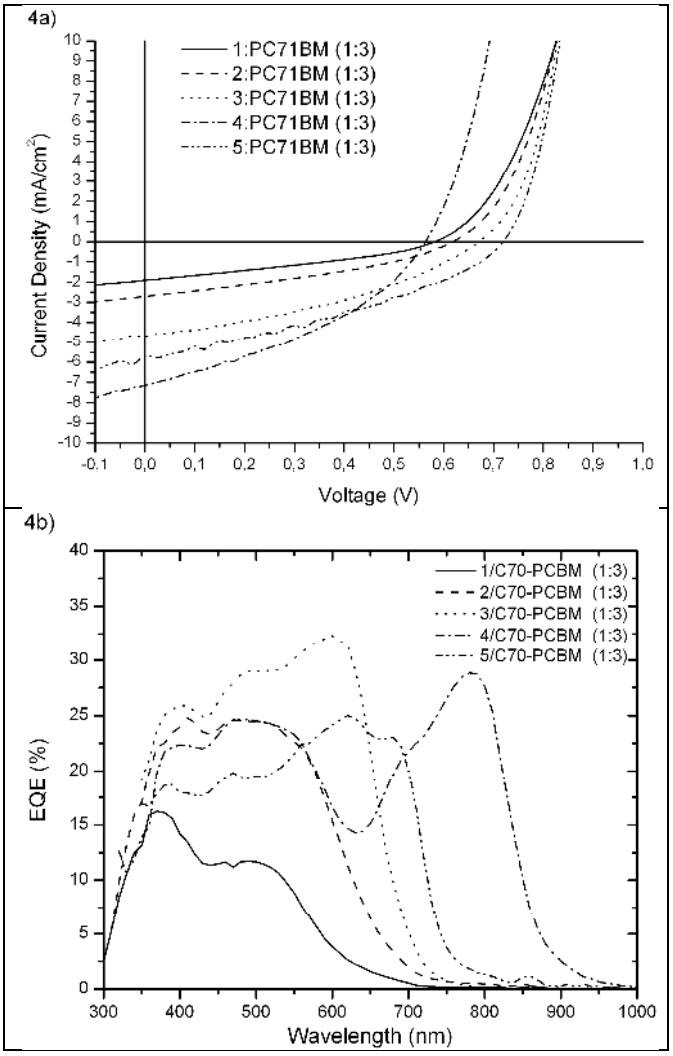

Figure 4. a) Average J-V response and b) External Quantum Efficiency of derivatives **1-5** and $PC_{71}BM$ based BHJ cells.

The only exception in the trend is represented by squaraine **3**. In fact, its electrochemical HOMO level is the lowest in the series, yet the Voc of the corresponding cell is slightly below that measured for derivative **5**. Such deviation is a consequence of the peculiar structure of 3. As we have mentioned before, the two hydrazones units of 3 are in meta position with respect to the electron deficient squarylium core, and hence only cross-conjugated. As a consequence, the radical cation formed upon oxidation cannot be efficiently delocalized over the whole molecule, as in the case of the other compounds. The oxidation process is not reversible and the error affecting the electrochemical estimate of the HOMO becomes larger. Also, the Fill Factor (FF) and the Short Circuit Current (Jsc) are relatively poor for all devices, likely as a consequence of limited hole mobility of these compounds.[29] Moreover, in the case of derivatives **1** and **2** the short circuit current is particularly low also due to the low molar absorbivity. We have already observed such effect in other hydrazone functionalized squaraine compounds we described in the past.[18] In this scenario the Voc value is significantly affected by factors not directly correlated with the difference in energy between the Donor HOMO and Acceptor LUMO.[30] The low FF values are also the reason for the relatively low efficiencies of derivatives **3** and **5**, which in principle are the most promising on judging from their absorption spectra and HOMO energies. The AFM analysis of the hydrazone/squaraine blend deposited on ITO/PEDOT substrate (Figure S1, Supporting Information) shows that morphology could also be a limiting factor for both compounds. The phase contrast images on best samples show that the new derivatives show poor connectivity in phase-separated domains, compared to the morphology afforded by the known compound 4.

In order to tackle this issue, we plan to further optimize derivatives **3-5** by changing the length and branching of the solubilizing alkyl chains. Nonetheless, as it is shown in Table 3, the most relevant result of this study consists in the capability to increase the cell Open Circuit Voltage by a progressive stabilization of the Donor HOMO energy.

Materials. All chemicals and solvents commercially available where purchased form Sigma-Aldrich chemical Co. and used as received. Derivatives 4,[24] 6,[25] 7,[31] 8,[32] 10[12] were prepared according to literature procedures.

(E)-1,2-bis(3,4-dibutoxy-5-((E)-(2,2-diphenylhydrazono)-methyl)thiophen-2-yl)ethane (1). A suspension of dialdehyde **6** (93 mg, 0.174 mmol) and diphenylhydrazine hydrochloride (76 mg, 0.348 mmol) in anhydrous THF (4 ml) is heated in a focused microwave oven under nitrogen atmosphere and in a pressurized vessel for 20 min at 200 W. Color turns red. The solvent is removed and the residue purified by chromatography (SiO_2, CH_2Cl_2) to give the pure product as a red bright solid (122 mg, 0.126 mmol, yield 76 %). ^{1}H NMR (500 MHz, $CDCl_3$): 7.44 (t, 8H,m J = 7.8 Hz), 7.31 (s, 2H), 7.20-7.15 (m, 12H), 7.01 (s, 2H), 4.01 (t, 4H, J = 6.6 Hz), 3.88 (t, 4H, J = 6.3 Hz), 1.74 (q, 4H, J = 7.8 Hz), 1.55-1.42 (m, 8H), 1.93 (m, 4H, J = 7.6 Hz), 1.01 (t, 6H, J = 7.4 Hz), 0.83 (t, 6H, J = 7.4 Hz). ^{13}C NMR (125.70 MHz, $CDCl_3$): 148.3, 147.0, 143.4, 129.8, 128.3, 125.7, 124.5, 122.4, 122.3, 116.7, 73.9, 73.8, 32.1, 31.8, 19.2, 19.0, 13.9, 13.8. Anal. Calcd for $C_{52}H_{60}N_4O_4S_2*H_2O$: C, 70.40; H, 7.04; N, 6.31. Found: C, 70.34; H, 7.01; N, 6.08.

1,3-bis(5-((E)-(2,2-diphenylhydrazono)methyl)thiophen-2-yl)benzo[c]thiophene (2). A suspension of dialdehyde **7** (50 mg, 0.140 mmol) and diphenylhydrazine hydrochloride (62 mg, 0.280 mmol) in anhydrous THF (4 ml) is heated in a focused microwave oven under nitrogen atmosphere and in a pressurized vessel for 30 min at 30 W. Color turns red. After addition of 36 mg of diphenylhydrazine hydrochloride, the mixture is heated at 50 W for 30 min. The solvent is removed and the residue purified by chromatography (SiO_2, CH_2Cl_2/light petroleum ether 3:4) to give the pure product as a deep red solid (80 mg, 0.116 mmol, yield 83 %). ^{1}H NMR (500 MHz, C_6D_6): 8.04 (dd, 2H, J=6.8,3.1), 7.36 (s, 2H), 7.20-7.15 (m, 8H), 7.13 (t, 8H, J = 8.7 Hz), 6.96 (d, 2H, J = 3.9 Hz), 6.93 (tt, 4H, J = 6.4, 3.85 Hz), 6.82 (dd, 2H, J = 7.0, 3.2),

6.39 (d, 2H, J = 3.9 Hz). ^{13}C NMR (125.70 MHz, C_6D_6): 144.4, 142.5, 136.6, 136.5, 130.9, 130.8, 128.9, 128.1, 126.2, 126.0, 125.5, 123.5, 122.8. Anal. Calcd for $C_{42}H_{30}N_4S_3$: C, 73.44; H, 4.40; N, 8.16. Found: C, 73.57; H, 4.78; N, 8.52.

5-((2,2-diphenylhydrazono)methyl)-1-octyl-1H-indole (9). A solution of derivative **8** (2.05 g, 6.65 mmol) is dissolved under nitrogen, atmosphere in 50 ml of anhydrous THF and the resulting colorless solution is cooled at -80 °C. A solution of 1.6 M BuLi in n-Hexane (5.0 ml, 8.00 mmol) is added dropwise and the resulting yellow solution is stirred at -80°C for 30 min. A solution of anhydrous DMF (1.23 ml, 1.17 g, 16.0 mmol) in THF (4 ml) is added dropwise and the resulting colorless solution is allowed to slowly warm up at room temperature. After 3 h stirring, the mixture is poured into 50 ml of 1 M HCl. The organic phase is separated, dried over Na_2SO_4 and the solvent evaporated to give a colorless viscous oil that was employed directly without further purification (1.23 g, 4.8 mmol, yield 72 %). ^{1}H NMR (500 MHz, $CDCl_3$): 10.03 (s, 1H), 8.16 (d, 1H, J = 1.0 Hz), 7.78 (dd, 1H, J = 8.6,1.4), 7.42 (d, 1H, J = 8.6 Hz), 7.19 (d, 1H, J = 3.2 Hz), 6.65 (d, 1H, J = 3.2 Hz), 4.15 (t, 2H, J = 7.2 Hz), 1.85 (quint, 2H, J = 7.1 Hz), 1.32-1.15 (m, 10H), 0.87 (t, 3H, J = 7.1 Hz). ^{13}C NMR (125.70 MHz, $CDCl_3$): 193.2, 140.2, 130.7, 130.1, 129.2, 127.3, 122.5, 110.8, 104.1, 47.5, 32.6, 31.1, 30.0, 27.8, 23.5, 15.0. The crude oil is dissolved in THF and diphenylhydrazine hydrochloride (1.25 g, 5.66 mmol) is added. The resulting suspension is refluxed under nitrogen atmosphere for 1 h. The solvent is removed and the residue is purified by chromatography (SiO_2, Et_2O) to give the product as yellow viscous oil. (1.01 g, 2.38 mmol, 42 % yield). ^{1}H NMR (500 MHz, DMSO-d_6): 7.67 (s, 1H), 7.57 (dd, 1H, J = 8.7, 1.3 Hz), 7.48 (t, 4H, J = 8.1 Hz), 7.47 (d, 1H, J = 9.4 Hz), 7.37 (d, 1H, J = 3.1 Hz), 7.25 (s, 1H), 7.22 (t, 2H, J = 7.4 Hz), 7.18 (d, 4H, J = 7.6 Hz), 6.42 (d, 1H, J = 3.0 Hz), 4.16 (t, 2H, J = 7.0 Hz), 1.74 (quint, 2H, J = 6.9 Hz), 1.30-1.15 (m, 10H), 0.84 (t, 3H, J = 7.0 Hz). ^{13}C NMR (125.70 MHz, DMSO-d_6): 144.9, 138.8, 131.3, 130.7, 129.5, 128.2, 125.5, 123.4, 120.9, 120.5, 111.5, 102.4, 56.2, 46.9, 32.5, 31.2, 30.0, 29.9, 27.6, 23.4, 15.2.

Squaraine 3. A suspension of hydrazone **9** (0.51 g, 1.20 mmol) and squaric acid (0.068 g, 0.6 mmol) in a 1:1 BuOH/toluene mixture (40 ml) is refluxed under a Dean-Stark trap. Color gradually turns from light yellow to deep violet. After 12 h at the reflux temperature, solvent is removed and residue taken up with EtOH (10 ml). The solid residue is filtered and crystallized from EtOH to give the pure title compound as a dark solid. (0.38 g, 0.41 mmol, 68 % yield). ^{1}H NMR (500 MHz, DMSO-d_6): 8.73 (s, 2H), 8.70 (s, 2H), 7.88 (dd, 2H, J = 8.6, 1.3 Hz), 7.69 (d, 8H, J = 8.6 Hz), 7.52 (t, 2H, J = 7.9 Hz), 7.38 (s, 1H), 7.27 (t, 4H, J = 8.7 Hz), 7.26 (d, 8H, J = 8.6 Hz), 4.41 (t, 4H, J = 7.2 Hz), 1.93 (quint, 4H, J = 6.8 Hz), 1.36 (s broad, 4H), 1.32-1.12 (m, 16H), 0.88 (t, 6H, J = 7.0 Hz). ^{13}C NMR (125.70 MHz, DMSO-d_6): 187.5, 144.8, 139.4, 139.0, 137.2, 133.1, 131.4, 131.2, 127.8, 126.0, 125.5, 124.5, 123.6, 123.4, 113.8, 112.3, 48.7, 32.4, 30.5, 29.8, 29.7, 27.4, 23.3, 15.1. Anal. Calcd for $C_{62}H_{64}N_6O_2$: C, 80.49 H, 6.97; N, 9.08. Calcd for $C_{62}H_{64}N_6O_2$ * ½ H_2O: C, 79.71; H, 7.01; N, 9.00. Found: C, 79.65; H, 6.85; N, 8.78.

3,6-bis(5-((E)-(2,2-diphenylhydrazono)methyl)thiophen-2-yl)-2,5-bis(2-ethylhexyl)pyrrolo[3,4-c]pyrrole-1,4(2H,5H)-dione (5). A suspension of dialdehyde **10** (200 mg, 0.34 mmol) and diphenylhydrazine hydrochloride (300 mg, 1.4 mmol) in THF (20 ml) is stirred at room temperature and in the dark for 12 h. The deep blue solution is evaporated to dryness to give a sticky residue that is purified by chromatography (SiO_2, CH_2Cl_2) yielding the title compound as a golden powder. (150 mg, 0.16 mmol, 48 % yield). ^{1}H NMR (500 MHz, C_6D_6): 9.67 (d, 2H, J = 3.9 Hz), 7.27 (s, 2H), 7.10 (t, 8H, J = 7.7 Hz), 7.06 (d, 8H, J = 7.8 Hz), 6.94 (t, 4H, J = 7.2 Hz), 6.46 (d, 2H, J = 3.8 Hz), 4.30-4.12 (m, 4H), 2.18 (quint, 2H, J = 5.8 Hz), 1.55-1.36 (m, 8H), 1.28 (s broad, 8H), 0.95 (t, 6H, J = 7.2 Hz), 0.87 (t, 6H, J = 6.5 Hz). ^{13}C NMR (125.70 MHz, C_6D_6): 162.5, 147.7, 143.9, 140.4, 137.8, 130.7, 130.3, 130.0, 128.9, 128.3, 125.9, 123.3, 110.1, 46.6, 40.6, 31.4, 29.2, 24.6, 24.1, 14.8, 11.3. Calcd for $C_{56}H_{60}N_6O_2S_2$: C, 73.65; H, 6.62; N, 9.20. Found: C, 73.59; H, 6.61; N, 9.09.

Identity and purity characterizations.

NMR spectra were recorded on a Bruker Avance 500 MHz spectrometer. UV-Vis spectra were recorded on a UV-Vis-NIR V-570 Jasco Spectrometer. Melting points were recorded on an Electrothermal apparatus and are uncorrected. Elemental analyses were performed by the Department of Geological Science of the University of Milano-Bicocca.

Details on electrochemical characterization.

Hydrazones were dissolved (concentration about 10^{-4} M) in the supporting electrolyte that was a 0.1 M solution of tetrabutylammonium hexafluorophosphate (Fluka, electrochemical grade, ≥99.0%) in anhydrous acetonitrile (Aldrich, 99.8%). Differential Pulsed Voltammetry (DPV) and Cyclic Voltammetry (CV) were carried out at scan rate of 20 and 50 mV/s, respectively, using a PARSTA2273 potentiostat in three electrodes electrochemical cell in a glove box filled with Argon ($[O_2] \leq 1$ ppm). The working, counter, and the pseudo-reference electrodes were a Au pin, a Pt flag and a Ag/AgCl wire, respectively. The Ag/AgCl pseudo-reference electrode was externally calibrated by adding ferrocene (1 mM) to the electrolyte.

Details on the preparation of OPV devices.

Compounds **1** and **2** were characterized at the University of Calabria according to the following details. Lithographically patterned ITO substrates (Unaxis, 110 nm thick, resistivity 12 Ω/□) were first cleaned by sequential ultra-sonications with soapy water, distilled water, acetone and isopropyl alcohol. Cleaned glasses were then transferred to a vacuum oven for overnight drying at 90 °C. The substrates were then treated with an air plasma (Diener Electronics, model Femto) at 100% plasma power, for 5 minutes. After being filtered with a 0.45 μm PVDF filter, a 50 nm thick layer (the thickness of the different layers was measured using DEKTAK 8 surface profiler) of polyethylenedioxythiophene : polystyrenesulphonate (PEDOT:PSS - Clevios P VP 4081 from H.C. Stark) was spin-coated at 1500 rpm for 90 sec, and dried at 200 °C for 10 minutes. Such substrates were then transferred to a glove box under Nitrogen atmosphere. Meanwhile, solutions of the Donor and $PC_{71}BM$ with a 1:3 weight ratio were prepared in different solvents (Dichloromethane, Chloroform, Chlorobenzene and Dichlorobenzene) and stirred overnight in the dark. In the glove box, the active layer was spin-coated on the PEDOT:PSS from such solutions (filtered with a 0.22 μm

PTFE filter) at 1400-1800 rpm for 60 sec. The coated substrates were then transferred to a thermal evaporator attached to the glove box for the evaporation of the LiF (Sigma-Aldrich, 99.995%) or Ca (Cerac, 99.5%) and Aluminium (KJ Lesker, 99.999%) electrode, at a base pressure of at least 10^{-7} Torr. The thicknesses were ~ 0.6-0.8 nm (or 20 nm) and ~ 200 nm for LiF (or Ca) and Al, respectively, and the growth rate was 1 Å/s for LiF and Ca, while for Al it was 1 Å/s for the first 50 nm and 1.5 Å/s up to 200 nm. The resulting overlap of the electrodes was 8.75 mm^2. Measurements of the I-V characteristics were performed in the glove box using a triple Class A solar simulator (SCIENCETECH, Model SS150W) and a Keithley 2400 source meter unit, by illuminating the samples without a mask at 100 mW/cm^2 (AM1.5G conditions). The solar simulator was calibrated by using a standard Si photodiode. Compounds **3**,**4** and **5** were characterized at the Polyera facility. Details are as follows. Devices were fabricated by spin-coating blends of squaraine + $PC_{71}BM$, sandwiched between a transparent anode and an Al cathode. The anode consisted of glass substrates pre-coated with indium tin oxide (ITO), modified by spin-coating with polyethylenedioxythiophene : polystyrenesulphonate (PEDOT:PSS) layer (~50 nm and ~75nm) as hole-transport, and the cathode consisted of lithium fluoride (~0.6 nm) capped with aluminum (~120 nm). Before device fabrication, the commercial ITO film on glass substrates (1.1mm) was patterned with aqueous HCl solution. The ITO-coated (150 nm thick films) glass substrates were then cleaned by ultrasonic treatment in aqueous detergent, deionized water, isopropyl alcohol, methanol, and acetone sequentially, and finally in a UV-ozone cleaner for 30 min under ambient atmosphere. In the meantime, a solution of PEDOT:PSS (Baytron VP) was used as a hole-transport layer, after filtration through a 0.45μm Teflon filter, and was used to spin-coat layers onto the ITO at 2000 rpm for 60 sec or 4000 rpm for 60 sec. Under a Petri dish in ambient atmosphere the sample was cured at 135 °C for 15 min. All blend solutions of squaraine + $PC_{71}BM$ were stirred for 1 h at 40 °C and then sonicated for 1 at 40 °C in the dark. The active layer was then obtained by spin-coating the blends at 5000 rpm for 30 sec in ambient atmosphere. Where necessary, sample areas for contacts were cleaned with chloroform and a cotton swab, and then transferred to the glove-box in nitrogen atmosphere for the electrode evaporation. The cathode growth rates used were 0.1 Å/s for LiF (Acros, 99.98%) and ~1.5 Å/s for Al (Sigma-Aldrich, 99.999%), with a chamber pressure of 1.1x10-6 Torr. The cathodes were deposited through a shadow mask with two 2mm strips perpendicular to the two patterned ITO (~3mm) strips to make four devices per substrate. Finally, the completed solar cells were encapsulated with a glass slide using UV-curable epoxy (Electro-Lite ELC- 2500), which was cured inside a UV chamber in the glove box.

Device evaluation was performed at 298 K using a Class A Spectra-Nova Technologies solar cell analyzer having a xenon lamp that simulates AM1.5G light from 400 – 1100 nm. The instrument was calibrated with a monocrystalline Si diode fitted with a KG3 filter to bring spectral mismatch to unity. The National Renewable Energy Laboratory (NREL) calibrated the calibration standard. Data are corrected for spectral mismatch. Four-point contacts were made to the substrate with copper alligator clips. A mask isolated individual devices during testing to avoid current collection from adjacent devices and edge effects. Atomic force microscopic (AFM) images were obtained using a JEOL-5200 Scanning Probe Microscope with silicon cantilevers in the tapping mode, using WinSPM Software.

Conclusions

We successfully synthetized and characterized a new series of end-capped diphenylhydrazone derivatives bearing a variety of electron withdrawing conjugated bridges. We demonstrated that it is possible to control the HOMO level energy of such derivatives by careful selection of the nature and substitution pattern of the electron withdrawing cores. Measurements in BHJ OPV cells using $PC_{71}BM$ as the Acceptor were carried out and exhibit PCEs up to ~1.5 %. Consistently with the energy of the HOMO levels of the various donor derivatives we employed, the cell Voc can be increased to a maximum of 0.74 V in the case of a diketopyrrolopyrrole core. This study shows that the diphenyl hydrazone moiety is a viable alternative to aromatic amines in Donor Acceptor dyes for photovoltaic applications. Further optimization of blend morphology and/or the use of different Accepting cores are expected to provide competitive conversion efficiencies.

Acknowledgements.

Financial support from the following agencies is gratefully acknowledged: European Community FP6 “Nanoeffect” and FP7 “Innoshade” grants; Fondazione Cariplo “ExPhon” 2011-1832 project.

Notes and references

[a] *Department of Materials Science and INSTM, University of Milano-Bicocca, Via Cozzi 53, I-20125 Milano, Italy.* [b] *Polyera Corporation, 8045 Lamon Avenue, Suite 140 ,Skokie, IL 60077.* [C] *Centro di Eccellenza CEMIF.CAL, LASCAMM CR-INSTM, CNR-IPCF UOS CS - LiCryL, Dipartimento di Chimica, Università della Calabria, 87036 Rende, Italy.*

† Electronic Supplementary Information (ESI) available: Copy of the ^1H and ^{13}C NMR spectra for all new compounds, DPV plots for derivatives **3** and **5**, AFM images of the blends, additional cells characterizations.

1. A. Mishra and P. Bäuerle, *Angew. Chem. Int. Ed.*, 2012, **51**, 2020–2067.
2. Y. Sun, G. C. Welch, W. L. Leong, C. J. Takacs, G. C. Bazan, and A. J. Heeger, *Nat. Mater.*, 2011, **11**, 44–48.
3. Y. Lin, Y. Li, and X. Zhan, *Chem. Soc. Rev.*, 2012, **41**, 4245–4272.
4. J. Peet, A. J. Heeger, and G. C. Bazan, *Accounts Chem. Res.*, 2009, **42**, 1700–1708.
5. C. J. Brabec, S. Gowrisanker, J. J. M. Halls, D. Laird, S. Jia, and S. P. Williams, *Adv. Mater.*, 2010, **22**, 3839–3856.
6. Z. He, C. Zhong, X. Huang, W.-Y. Wong, H. Wu, L. Chen, S. Su, and Y. Cao, *Adv. Mater.*, 2011, **23**, 4636–4643.
7. L. Dou, J. You, J. Yang, C.-C. Chen, Y. He, S. Murase, T. Moriarty, K. Emery, G. Li, and Y. Yang, *Nature Photon*, 2012, **6**, 180–185.
8. G. Li, R. Zhu, and Y. Yang, *Nature Photon*, 2012, **6**, 153–161.
9. J. M. Szarko, J. Guo, B. S. Rolczynski, and L. X. Chen, *J. Mater. Chem.*, 2011, **21**, 7849–7857.
10. C. Kim, J. Liu, J. Lin, A. B. Tamayo, B. Walker, G. Wu, and T.-Q. Nguyen, *Chem. Mater.*, 2012, **24**, 1699–1709.
11. S. Qu and H. Tian, *Chem. Commun.*, 2012, **48**, 3039–3051.
12. B. P. Karsten, J. C. Bijleveld, and R. A. J. Janssen, *Macromol. Rapid Commun.*, 2010, **31**, 1554–1559.

13. S. Loser, C. Bruns, H. Miyauchi, R. Ponce Ortiz, A. Facchetti, S. Stupp, and T. Marks, *J. Am. Chem. Soc.*, 2011, **133**, 8142–8145.
14. S. Steinberger, A. Mishra, E. Reinold, J. Levichkov, C. Uhrich, M. Pfeiffer, and P. Bäuerle, *Chem. Commun.*, 2011, **47**, 1982–1984.
15. G. Ren, E. Ahmed, and S. Jenekhe, *J. Mater. Chem.*, 2012.
16. G. Ren, E. Ahmed, and S. Jenekhe, *Adv. Energy Mater.*, 2011.
17. D. Bagnis, L. Beverina, H. Huang, F. Silvestri, Y. Yao, H. Yan, G. A. Pagani, T. J. Marks, and A. Facchetti, *J. Am. Chem. Soc.*, 2010, **132**, 4074–4075.
18. L. Beverina, M. Drees, A. Facchetti, M. Salamone, R. Ruffo, and G. A. Pagani, *Eur. J. Org. Chem.*, 2011, **2011**, 5555–5563.
19. U. Mayerhöffer, K. Deing, K. Gruss, H. Braunschweig, K. Meerholz, and F. Würthner, *Angew. Chem. Int. Ed.*, 2009, **48**, 8776–8779.
20. H. Bürckstümmer, E. V. Tulyakova, M. Deppisch, M. R. Lenze, N. M. Kronenberg, M. Gsänger, M. Stolte, K. Meerholz, and F. Würthner, *Angew. Chem. Int. Ed.*, 2011, **50**, 1–6.
21. J. Meiss, A. Merten, M. Hein, C. Schuenemann, S. Schäfer, M. Tietze, C. Uhrich, M. Pfeiffer, K. Leo, and M. Riede, *Adv. Funct. Mater.*, 2011, **22**, 405–414.
22. C. Schünemann, D. Wynands, L. Wilde, M. Hein, S. Pfützner, C. Elschner, K.-J. Eichhorn, K. Leo, and M. Riede, *Phys. Rev. B*, 2012, **85**, 245314–1–10.
23. F. Silvestri, I. López-Duarte, W. Seitz, L. Beverina, M. V. Martínez-Díaz, T. J. Marks, D. M. Guldi, G. A. Pagani, and T. Torres, *Chem. Commun.*, 2009, 4500–4502.
24. F. Silvestri, M. D. Irwin, L. Beverina, A. Facchetti, G. A. Pagani, and T. J. Marks, *J. Am. Chem. Soc.*, 2008, **130**, 17640–17641.
25. S. Zheng, A. Leclercq, J. Fu, L. Beverina, L. A. Padilha, E. Zojer, K. Schmidt, S. Barlow, J. Luo, S.-H. Jiang, A. K.-Y. Jen, Y. Yi, Z. Shuai, E. W. Van Stryland, D. J. Hagan, J.-L. Brédas, and S. R. Marder, *Chem. Mater.*, 2007, **19**, 432–442.
26. A. Ajayaghosh, *Accounts Chem. Res.*, 2005, **38**, 449–459.
27. H. J. Son, F. He, B. Carsten, and L. Yu, *J. Mater. Chem.*, 2011, **21**, 18934–18945.
28. L. Beverina, M. Crippa, P. Salice, R. Ruffo, C. Ferrante, I. Fortunati, R. Signorini, C. M. Mari, R. Bozio, A. Facchetti, and G. A. Pagani, *Chem. Mater.*, 2008, **20**, 3242–3244.
29. M. Binda, A. Iacchetti, D. Natali, L. Beverina, M. Sassi, and M. Sampietro, *Appl. Phys. Lett.*, 2011, **98**, 073303–1–073303–3.
30. M. D. Perez, C. Borek, S. R. Forrest, and M. E. Thompson, *J. Am. Chem. Soc.*, 2009, **131**, 9281–9286.
31. A. K. Mohanakrishnan, M. V. Lakshmikantham, C. McDougal, M. P. Cava, J. W. Baldwin, and R. M. Metzger, *J. Org. Chem.*, 1998, **63**, 3105–3112.
32. M.-L. Go, J. L. Leow, S. K. Gorla, A. P. Schüller, M. Wang, and P. J. Casey, *J. Med. Chem.*, 2010, **53**, 6838–6850.